DESIGN AND DEVELOPMENT OF COMPACT MICROSTRIP ANTENNAS FOR PORTABLE DEVICE APPLICATIONS

[1]Ahmed Toaha Mobashsher, [2]Mohammad Tariqul Islam, [1]Norbahiah Misran

[1]Dept. of Electrical, Electronic and Systems Engineering, Universiti Kebangsaan Malaysia, Bangi, Selangor, Malaysia
[2]Institute of Space Science (ANGKASA), Universiti Kebangsaan Malaysia, Bangi, Selangor, Malaysia

Key words: HCASA, SSA, COMPACT ANTENNA, portable device applications

Abstract: During the last decade, wireless communication system developments have been a major motivator of compact antenna research, most particularly for portable device applications. This paper addresses to a development procedure of designing compact antennas. By a careful observation at the current distribution and folding of slots after calculating the resonating slot length, the compactness of microstrip antenna can be achieved. Two compact slot antennas, namely hollow central annular slot antenna (HCASA) and spiral slot antenna (SSA) are designed and prototyped for validation, where the experimental result agrees well the simulation. The overall volume of these antennas are respectively $0.11\lambda_o \times 0.11\lambda_o \times 0.005\lambda_o$ and $0.08\lambda_o \times 0.08\lambda_o \times 0.005\lambda_o$ where λ_o is the free space operating wavelength, that concludes the reduction of 75 and 86.2% of antenna volume comparing that of an ordinary annular slot antenna operating at the same frequency.

Načrtovanje in razvoj kompaktnih mikrostrip anten za uporabo v prenosnih napravah

Kjučne besede: HCASA, SSA, kompaktna antena, uporaba za prenosne naprave

Izvleček: Razvoj brezžičnih komunikacijskih sistemov je v zadnjem desetletju bil glavna gonilna sila razvoja kompaktnih anten večinoma za uporabo v prenosnih naprav. V članku je opisan postopek razvoja načrtovanja kompaktnih anten do katerih pridemo z analizo tokovne porazdelitve ter rezonančne dolžine in položaja rež. Načrtali in probali smo dva tipa kompaktnih anten z režami, kjer se simulacije ujemajo z eksperimentalnimi rezultati: HCASA – antena s sredinskim obročem in SSA – spiralna antena.

Prostornini teh anten so $0.11\lambda_o \times 0.11\lambda_o \times 0.005\lambda_o$ in $0.08\lambda_o \times 0.08\lambda_o \times 0.005\lambda_o$, kjer λ_o predstavlja valovno dolžino v vakumu; to pomeni zmanjšanje za 75% in 86,2 % volumna navadnih anten, ki delujejo na enaki frekvenci.

1. Introduction

In modern mobile and wireless communications systems, there is a increasing demand for compact antennas that can be easily integrated into the portable devices. In this regard, microstrip antennas are highly preferred because of their characteristics such as ease of fabrication and integration, compactness and low profile. Basically the compactness of the antenna is a trade-off between the size and the performance of the antenna due to the fact that antenna performance is bound with the fundamental limits based on the size of the antenna. This is especially true in the field of radio communications, where reducing the size of an antenna leads to smaller and light-weight systems, thereby enhancing portability and minimizing electromagnetic interference with other electronic devices.

One way for miniaturization is to alter the geometry of the antenna, such that the electrical length of the current path is increased /1/. Nevertheless, the size of microstrip patch antenna can be reduced with a dielectric of the high relative dielectric constant. But the dielectric caused the degradation of gain and radiation efficiency, thus we need to develop methods for miniaturization through the structural change of the patch.

There are some methods reported to minimize the antenna resonating at some lower frequencies. It has been shown that resonant patch antennas can be miniaturized using artificial magneto dielectrics /2/. Further compactness of these antennas has also been achieved through loading, using dielectrics, resistors, shorting pins, or meandering microstrip lines /3/. However, such loadings can increase their loss, complication or fabrication cost. In portable devices there is PIFA, IFA and printed monopole or loop antennas are very promising and widely used as compact antennas /4-6/.

However, such internal mobile antennas usually excite large surface currents on the system ground plane of the mobile phone, which functions as an effective radiation portion. An isolation distance of about $7mm$ or larger between the antenna and the nearby conducting elements or electronic components in the mobile phone is usually required to avoid large degradation effects on the performances of the internal antenna, due to the large excited surface currents

Informacije MIDEM 41(2011)2, str. 105-113

A. T. Mobashsher, M. T. Islam, N. Misran:
Design and Development of Compact Microstrip Antennas for ...

on the system ground plane, especially in the region near the internal antenna /7,8/.This is a big limitation for the portable devices.

In this paper, a design procedure of compact antennas is proposed which is based on calculating the resonating slot length. The process starts from a conventional annular ring slot antenna and ends with two proposed compact antennas. All of the antennas are designed for operation at 920 MHz. On the basis of the current distribution, it has been shown that the antenna slots can also be folded or coiled in spiral to produce lower frequencies in a low profile by maintaining almost the same slot length. However some impedance matching measures has to be taken to optimize the antennas in desired low frequencies. From the view of simplicity and compactness, these miniaturized antennas are also very prognosticating as they do not need big ground planes to provide good radiation patterns.

2. Theoretical evaluation

Slot antennas are attractive because they are easy to analyze, design and fabricate. Their radiation pattern can be bidirectional or unidirectional and is possible to have radiation at low elevation angles for an annular slot of the geometry shown in the co-ordinate system of Figure 1 in an infinite and perfectly conducting ground plane, magnetic surface current of the annular distribution can be given by

$$\vec{M}(\rho,\phi') = \vec{E}_a(\rho,\phi').\hat{n}$$

where E_a is the aperture electric field and $\hat{n}$ is the unit vector normal to the aperture.

The general equations for the-far electric field components E_θ and E_ϕ can be written as /9/

$$E_\theta = \frac{-jk}{4\pi} \frac{e^{-jkR}}{R} \int_0^{2\pi} \int_a^{a+W} \{M(\rho)\sin(\phi'-\phi) +$$

$$+ M(\phi'-\phi)\}.e^{j\rho k\sin\theta\cos(\phi'-\phi)}.\rho d\rho d\phi'$$

$$E_\phi = \frac{jk}{4\pi} \frac{e^{-jkR}}{R}.\cos\theta.\int_0^{2\pi} \int_a^{a+W} \{M(\rho)\cos(\phi'-\phi) +$$

$$+ M(\phi')\sin(\phi'-\phi)\}.e^{j\rho k\sin\theta\cos(\phi'-\phi)}.\rho d\rho d\phi'$$

where k is the free space propagation constant.

Let us consider the point of observation P is represented in the co-ordinate by R, Θ and ϕ; the inner radius of the annular slot as a; the width of the slot as W and

$$\vec{M}(\rho,\phi') = -E_\phi\,\hat{\rho} + E_\rho\,\hat{\phi}$$

where E_ϕ and E_ρ are respectively the slot electric field components in ϕ and Θ directions. For a narrow ($W \ll \lambda_0$) and fixed annular slot the field component equations can be solved as
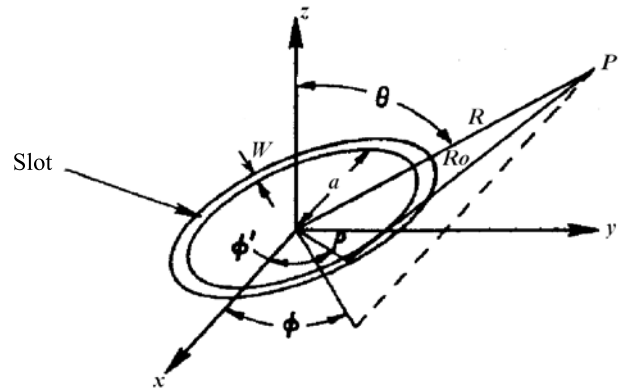

Fig. 1.   Annular-slot Geometry

$$E_\theta = -j^n E_o a \frac{kW}{2} \frac{e^{-jkR}}{R} \cos n\phi.J_n'(ak\sin\theta)$$

$$E_\phi = j^n nE_o a \frac{W}{2} \frac{e^{-jkR}}{R} \sin n\phi.\cot\theta.J_n(ak\sin\theta)$$

where $J_n'(ak\sin\theta) = \dfrac{d}{d(ak\sin\theta)}J_n(ak\sin\theta)$

However, for a constant slot width and when $0.0015 \leq w/\lambda_0 \leq 0.075$ and $3.8 \leq \varepsilon_r \leq 9.8$ an approximation can be provided to obtain the guided wavelength of the resonance by using Bessel functions as /10/

$$\lambda_g = \lambda_o \left[0.9217 - 0.277\ln(\varepsilon_r) + 0.0322\left(\frac{w}{h}\right)\left(\frac{\varepsilon_r}{\frac{w}{h}+0.453}\right)^{0.5} - \right.$$

$$\left. - 0.01\ln\left(\frac{h}{\lambda_o}\right)\left\{4.6 - \frac{3.65}{\varepsilon_r^2 \sqrt{w/\lambda_o}\left(9.06-100 w/\lambda_o\right)}\right\} \right]$$

Nevertheless, the dominant TM_{n1} mode resonant frequency, f_n of the slot antenna is determined by

$$f_n = \frac{nc}{2\pi \sqrt{\varepsilon_{eff}}\left(R_m/2\right)}$$

Here, R_m is the mean radius of the annular ring slot, n is the mode number of resonance, ε_{eff} is the relative efficiency of the slot line and c is the speed of light in free space. Usually, the resonant frequencies are mainly determined by the mean radius of the annular slot. The mean radius can be defined by $R_m = (R_i + R_0)/2$ where, R_i is the inner radius and R_0 is the outer radius of the annular ring slot.

3. Antenna miniaturization

In order to explain the miniaturization technique of the microstrip antenna using current distribution trace, a conventional annular ring slot microstrip antenna has been discussed with a center frequency of 920MHz, shown in Figure 2. The antenna is designed on FR4 substrate of $\varepsilon_r = 4.4$ and $tan\delta = 0.02$. The antenna dimensions are tabulated

A. T. Mobashsher, M. T. Islam, N. Misran:
Design and Development of Compact Microstrip Antennas for ...

Informacije MIDEM 41(2011)2, str. 105-113

in Table I. A symmetrical external 50Ω microstrip feeding is introduced to provide impedance matching and excite the conventional annular ring slot. As the fundamental TM_{11} mode is excited the corresponding equation to determine resonance can be found as

$$f = \frac{c}{2\pi \sqrt{\varepsilon_{eff}} \left(\frac{R_o + R_i}{2} \right)}$$

It is noted that this equation is valid as long as a thin substrate is used for the annular ring antenna.

Table 1 Design parameters of the conventional annular slot antenna

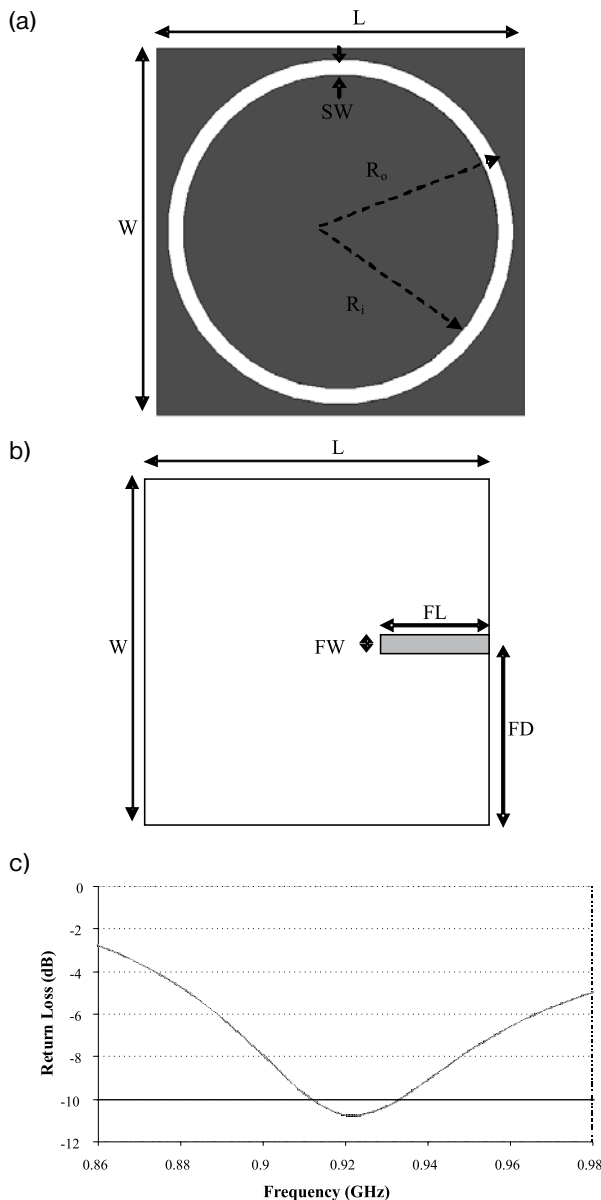| L	W	R_o	R_i	SW	FW	FL	FD
70	70	33	30	3	3	16	35

(a)

b)

c)

Fig. 2. The (a) top view, (b) bottom view and (c) return loss of conventional annular slot antenna
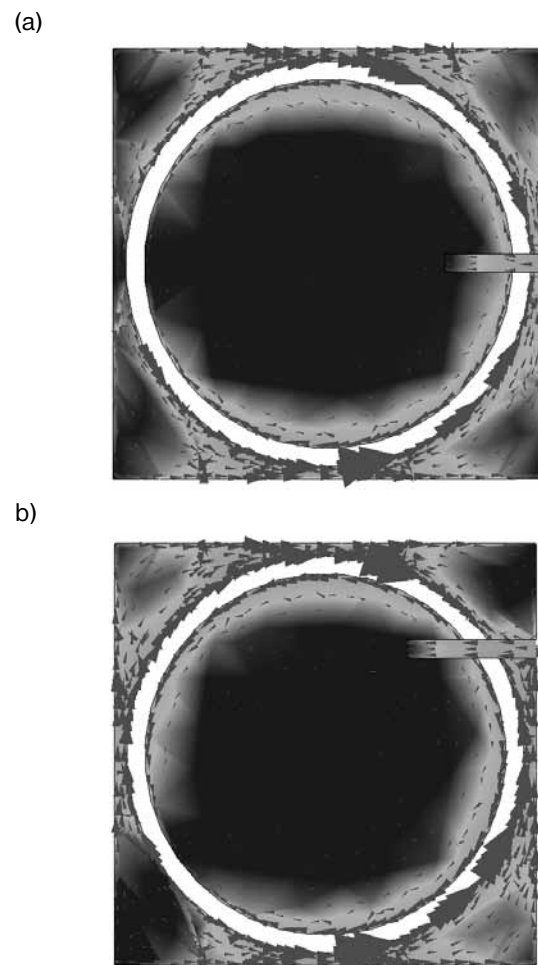
(a)

b)

Fig. 3. Current distribution at 920MHz of (a) conventional annular ring slot antenna and (b) annular ring slot antenna with side feeding

As presented in Figure 2(b), the antenna shows a -10 dB bandwidth of 18.2 MHz having central frequency of 920 MHz. In order to understand the effect of the antenna feeding position, the feeding is displaced from the middle to FD = 52.5 *mm*. Providing proper impedance matching by varying the feeding length, the modified antenna achieves resonance at 920MHz. As seen from the current distribution pattern of the antennas in Figure 3, at resonance frequency, the current densely flows at the edges of the annular slots, while in middle portions of the circular disks the currents are null. The current flows toward the microstrip feeding at the outside portion of the slot and at the inside portion of the slot the current traces flows from the feeding. These two traces produce null current at mean slot length of about $2\pi R_m/2 \approx 0.5\lambda_g$ where guided wavelength at resonance frequency, $\lambda_g = \lambda / \sqrt{\varepsilon_{eff}}$ and effective dielectric constant $\varepsilon_{eff} \approx \frac{(\varepsilon_r + 1)}{2} = 2.7$; which makes the current paths symmetrical to the microstrip feeding line /11/.

Shifting the antenna feeding line in the upper portion of the antenna increases current density in that region. This introduces the initial step of miniaturization, by cutting the modified antenna in the middle and taking the high
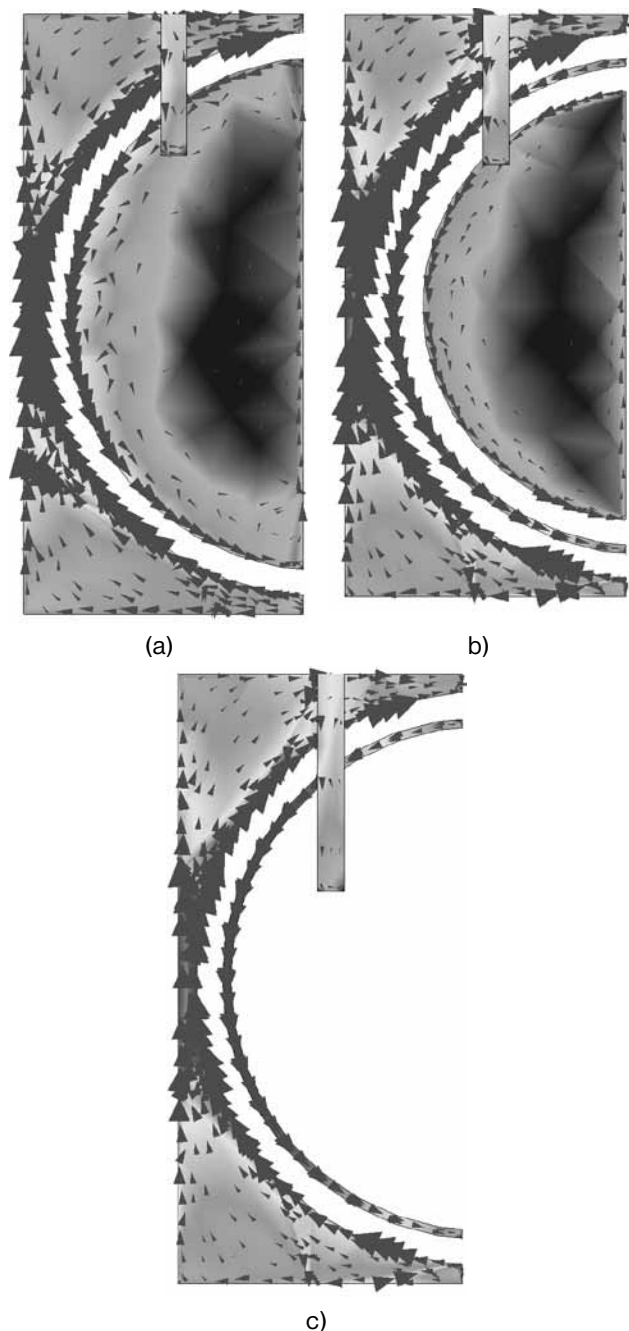
(a)   b)

c)

Fig. 4. *Current distribution at 920MHz of (a) half annular ring slot antenna (b) half double annular ring slot antenna and (c) half double annular ring slot antenna without central disk*

current density portion into account, which is pictured in Figure 4(a). Moreover, in order to match the impedance accurately 2.5mm width is shorten from the half circular antenna, which makes the mean circumference of the antenna $\approx (2 \cdot \pi \cdot 31.5)/2 - 2 \cdot 2.5 \approx 0.47\lambda_g$ where λ_g is the wavelength at the slot at the resonance frequency. This resolves that the minimized slot antenna fed by a microstrip transmission line radiates as a magnetic dipole /12/. Nevertheless, it is exhibited that the current density largely flows on the two edges of the dipole like slot and in the central portion of the antenna current strength gradually decreases. So as the next step of miniaturization, shown

in Figure 4(b), another half ring slot of 2mm is cut on the ground plane providing 1mm distance between the slots. This half double annular ring slot antenna (HDARSA) also resonates at the desired frequency of 920MHz. However, this also shows null current traces in the central portion of the disk. So for the sake of miniaturization, in the next step, depicted in Figure 4(c), the half circular disk is etched from the ground and it was observed that the current distribution remains almost similar. However, the length of feeding line is extended for better impedance matching in the resonating frequency. In the following sections two miniaturized antennas are proposed and their optimization process is presented and discussed.

4. Proposed geometry description

The configurations of the two compact microstrip slot antennas are illustrated in Figure 5. Both of the antennas are designed on a low cost substrate, FR4 of height $h_s = h_c$ =1.6mm with relative permittivity ε_r = 4.4 and loss tangent $tan\delta$ =0.02. The first antenna is a hollow central annular slot antenna (HCASA), which consists of an annular slot with the central portion etched out from the ground of antenna. And second spiral slot antenna (SSA) having an optimized spiral slot in the ground plane. Both of the antennas are fed by 50Ω microstrip lines, which give suitability for the antennas to embed with the circuit boards. The antenna design parameters of the microstrip-fed miniaturized antennas are given in Table II. In Table III the comparative volume of the miniaturized antennas are also mentioned.
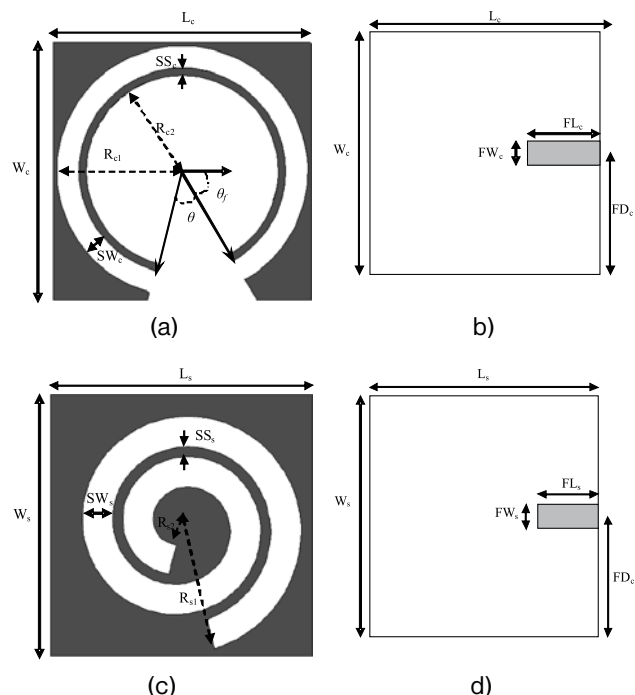

(a)   b)

(c)   d)

Fig. 5. *Structure of proposed hollow central annular slot antenna (HCASA) top and side view (a & b), spiral slot antenna (SSA) top and side view (c & d)*

Table 2: Design parameters of the miniaturized antennas

Hollow Central Annular Slot Antenna (HCASA)	L_c	W_c	R_{c1}	R_{c2}	SW_c	SS_c	FW_c	FL_c	FD_c	θ	θ_f
	35	35	17	14	3	1	3	10	17.5	45	60

Spiral Slot Antenna (SSA)	L_s	W_s	R_{s1}	R_{s2}	SW_s	SS_s	FW_s	FL_s	FD_c
	26	26	11.7	2	3	1	3	7	13

Table 3: Comparative volume of the miniaturized antennas

	Hollow Central Annular Slot Antenna (HCASA)	Spiral Slot Antenna (SSA)
Antenna Volume (mm)	35×35×1.6	26×26×1.6
Antenna Volume Relative to the Free Space Operating Wavelength (λ_o)	0.11 λ_o ×0.11 λ_o ×0.005 λ_o	0.08 λ_o ×0.08 λ_o ×0.005 λ_o

5. Analytical study & optimization

The goal of the performed analytical parametric studies is to facilitate more elaboration of the design procedures and optimization processes for miniaturized antennas. Various parameters are investigated to examine the effects of the antenna parameters on resonant frequency, return loss as well as the impedance bandwidth of the antenna. This study covers the formulation of the antenna design, influences of varying the slot lengths on resonant frequency and return loss, the implication of choosing the separation angle for the design, the consequence of changing the offset angle for achieving the best optimized minimized antennas. For better convenience of the effect on the performance of the antenna upon changing the parameters, only one parameter is changed at a time, while keeping others unchanged.

5.1. HCASA

The mean circumference of the HCASA slot can be illustrated as, $C(\Theta) = 2\pi \cdot r - \Theta \cdot r$

Applying this equation for the designed antenna we get, for $\Theta = \pi/8$ and $r = 15.5$, the length $C(\Theta) = 91$. The length of the circular slot is approximately $0.46\lambda_g$, where λ_g is the wavelength at the slot at the resonance frequency. This properly corresponds to the miniaturized half circular antennas discussed previously discussed. Nevertheless, the angles for the two ends of the slots are optimized to achieve proper impedance matching for the best performance of the antenna.

Figure 6 shows the relationship between the angle of separation, Θ between the two edges of the slot with the resonant frequency and return loss at the respective frequency. It is seen that the resonant point of the antenna increases almost linearly when the angle, Θ is increased gradually. In the same time, the respective return loss does not behave so monotonously. This is because of the impedance matching of the antenna with feeding strip. In spite of the ripples we can derive a merely straight line for the relation of Θ and return loss. However it is also observed

(not shown in graph) that the bandwidth of the antenna increases with increase of the angle. The reason for this phenomenon can be attributed to the relatively electrically large aperture of the antenna as the resonance frequency also increases, having the physical dimensions of the overall patch remaining almost the same. In this design, the angle, $\Theta = 45°$ is taken as the optimized one for attaining the resonance frequency of 920MHz.
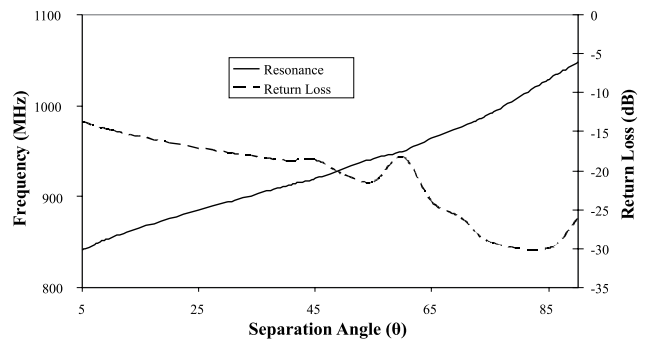

Fig. 6. The effect of different separation angel, Θ on resonant frequency and return loss
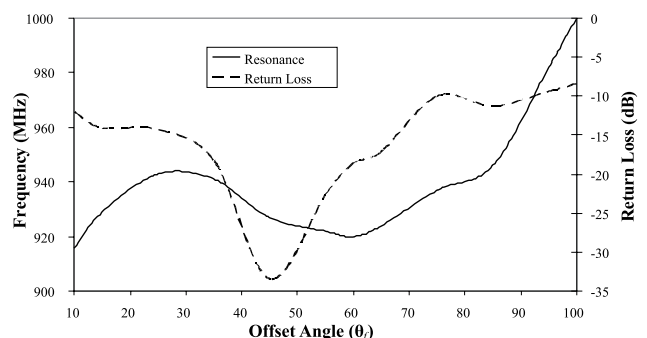

Fig. 7. The relationship between the offset angle, Θ_f with resonance and return loss

The offset angle of the slot edge, Θ_f from the line of feeding affects the impedance matching and the resonance frequency dramatically, which is verified by the exhibited graphs of Figure 7 with different values of Θ_f angle providing other shapes and parameters unchanged. Figure 9 shows

that the antenna meets the desired resonance frequency 920MHz when $\Theta_f \approx 10°$ with a low return loss, which implies a defective impedance matching of the antenna. However the best impedance matching is achieved when $\Theta_f = 45°$ but the resonating frequency is over 920MHz. When $\Theta_f = 60°$, the resonance falls once again at 920MHz with a better impedance matching and this is taken as the optimized parameter. Nevertheless, with the increasing of when Θ_f, the resonance point still goes to higher frequencies with a gloomy return loss.

5.2. SSA

Spiral arm can be represented as /13/, $r(\varphi) = a\,\varphi + r_a$, $(\varphi_s < \varphi < \varphi_e)$

Here, $r(\varphi)$ is the radial distance from the origin to the arbitrary point on the centre line of the spiral, a is the spiral constant, φ is the winding angle, φ_s is the spiral start angle, φ_e is the spiral end angle, and r_a is the radial distance from the origin to the initial point of the spiral line.

The mean arc length of the Archimedean spiral $C(\varphi_s, \varphi_e)$ in polar coordinates between φ_s and φ_e is:

$$C(\varphi_s, \varphi_e) = a \int_{\varphi_s}^{\varphi_e} \sqrt{1 + \varphi^2}\, d\varphi \tag{1}$$

However, from calculus formula, for the simplification of a variable φ representing the angle in radians staring from $\varphi = 0$ radians and wrapping counter clockwise around pole until angle $\varphi = \varphi_e$ radians it can be derived:

$$\int_{\varphi_s}^{\varphi_e} \sqrt{1 + \varphi^2}\, d\varphi = \frac{1}{2}\left[\varphi\sqrt{1+\varphi} + \ln\left(\varphi + \sqrt{1+\varphi^2}\right) \right]_{\varphi_s}^{\varphi_e}$$

It reveals equation (1) as follows:

$$C(\varphi_s, \varphi_e) = \frac{1}{2}\left[\varphi\sqrt{1+\varphi} + \ln\left(\varphi + \sqrt{1+\varphi^2}\right) \right]_{\varphi_s}^{\varphi_e} \tag{2}$$

Where, for the proposed Archimedean spiral antenna, $\varphi_s = 1.17\pi$ and $\varphi_e = 2.56\varpi$. Solving equation (2), the length of the arc is attained as $90.91\,mm$. This is also approximately corresponds to $0.046\lambda_g$, where λ_g is the guided wavelength at 920MHz. This proves that the proposed miniaturized spiral antenna slot acts like a magnetic dipole for the resonating frequency. In the next section the effect of the mean spiral length is discussed for the better understanding of the antenna geometry.

Figure 8 exhibits the relationship between the mean slot length with the resonant frequency and input impedance of the antenna. It is seen from Figure 8 that resonant frequency is a linear function of the slot length until the spiral slot meets the edge of the antenna. When the slot length crosses over 109mm, the slot can not be confined in the antenna surface; it cuts the edge of the antenna, which introduces a discontinuity to the return path of current components and acts like a monopole slot antenna and resonates at a lower frequency. However the impedance bandwidth of the antenna decreases due to the relatively low profile of the antenna at that frequency. The input impedance characteristics of the antenna are not so linear; but also do not vary rapidly as the slot length is increased. On the other hand as the Archimedean spiral slot length decreases the antenna resonance point increases following the $\approx 0.46\,\lambda_g$ approximation. In this case, the resistance of the real part and capacitive effect of the imaginary portion of the input impedance increases; which also reduces the return loss and impedance bandwidth of the antenna. The characteristics of the antenna with the varying slot length are summarized in Table V. When the slot length is about 92mm then the antenna resonates at 920MHz and shows the best impedance matching where the input reactance exhibits the highest inductance. This also results the highest -10dB bandwidth for the proposed spiral slot antenna /14/.

Table 4: Characteristics of the antenna with varying slot length

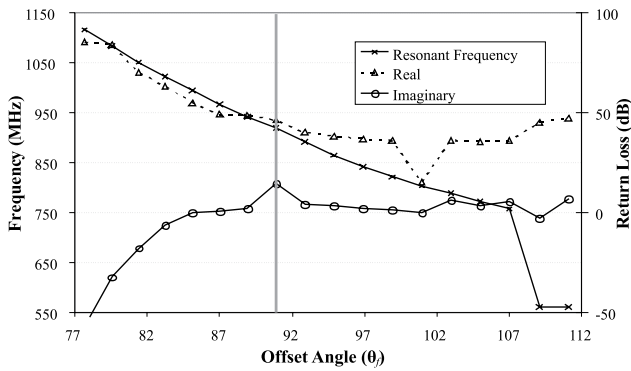| Slot Length (mm)	Resonant Frequency (MHz)	Antenna length or width (26mm) relative to free space wavelength (λ_o)	Return Loss (dB)	Bandwidth with below -10dB (MHz)	Input Impedance	
					Real (ohm)	Imaginary (moh)
77.68	1116	$0.097\,\lambda_o$	-6.8	-	85.5	-57.2
79.55	1084	$0.094\,\lambda_o$	-9.29	-	84.4	-32.4
81.39	1052	$0.091\,\lambda_o$	-13	3	70.13	-17.81
83.24	1023	$0.089\,\lambda_o$	-17.62	3.7	63.4	-6.34
85.12	994	$0.086\,\lambda_o$	-26.26	4.71	55.1	-0.2
87	968	$0.084\,\lambda_o$	-38.62	9.25	49.2	0.85
88.92	943	$0.082\,\lambda_o$	-24.6	9.3	48.8	2.1
90.91	*920*	*$0.080\,\lambda_o$*	*-16.2*	*11.2*	*46.2*	*14.5*
92.87	892	$0.077\,\lambda_o$	-18.4	9.1	40.14	3.88
94.87	865	$0.075\,\lambda_o$	-17.1	8.93	38.2	3.22
96.88	841	$0.073\,\lambda_o$	-16.4	8.87	36.94	1.88
98.9	821	$0.071\,\lambda_o$	-15.77	8.6	36.1	1.54
100.93	804	$0.070\,\lambda_o$	-15.51	8.3	15	0.07
102.93	788	$0.068\,\lambda_o$	-15.1	8.1	36.3	6.25
104.98	772	$0.067\,\lambda_o$	-15.1	7.9	35.53	3.59
106.98	757	$0.065\,\lambda_o$	-15.1	7.8	35.95	5.55
109.05	560	$0.049\lambda_o$	-24.52	6.2	45.23	-2.97
111.05	560	$0.049\,\lambda_o$	-22.23	6	47.3	7.02

Fig. 8.   The effects of various slot lengths on resonant frequency and input impedance (real & imaginary) of SSA

6.   Results & discussions

The proposed hollow central annular slot antenna (HCASA) and spiral slot antenna (SSA) are prototyped for the verification and measured using Agilent E9362C network analyzer. It was seen that the measured results agrees the simulated results. The prototypes are shown in figure 9.

Fig. 9.   Fabricated Prototype of the designed antennas shown in Figure 5

The measured and simulated return losses of the proposed hollow central annular slot antenna (HCASA) and spiral slot antenna (SSA) are illustrated in Figure 10. The measured return loss curve shows that both of the proposed antennas are excited at 920MHz. HCAS antenna shows a –10 dB return-loss bandwidth of 16.2MHz (910–930 MHz) and SS antenna exhibits an impedance bandwidth of 11.2MHz (909–927GHz). The maximum return loss of -22dB and -19.5dB is obtained at the resonant frequencies of HCASA and SSA respectively. The slight degradations of bandwidth are in accordance with the well known classical fundamental limits of electrically small antennas /15/.

The E and H plane radiation patterns of the proposed HCASA and SSA at 920MHz has been shown in Figure 11. Both of the antennas produce omni-directional radiation patterns. For HCASA, in E and H-plane the cross-polarization value is below *24dBi*, while for SSA it increases to *15dBi*. This is due to the extremely low volume of the antenna with
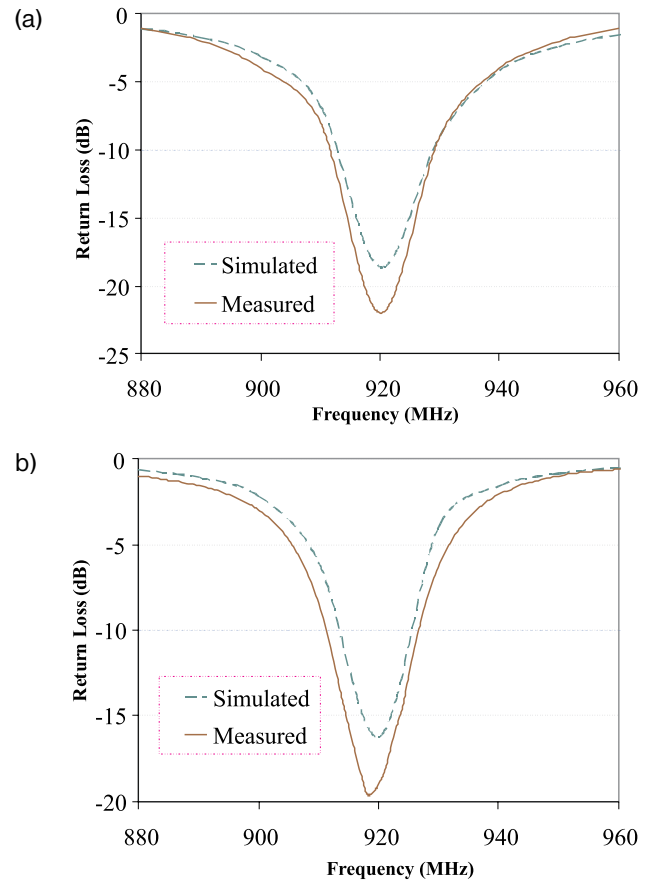

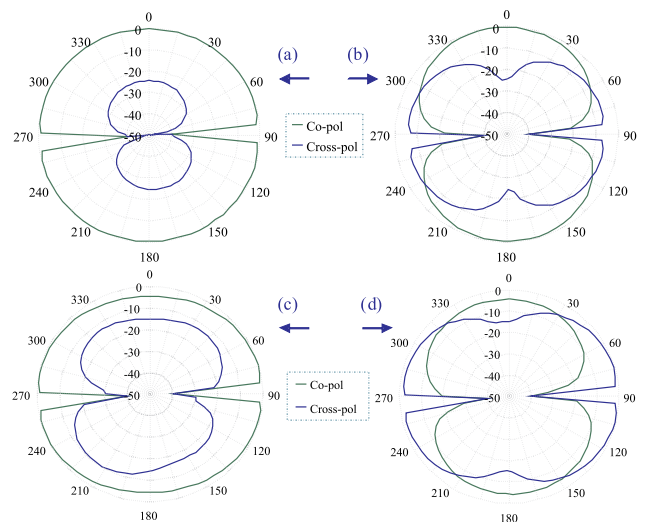Fig. 10.   The return losses of (a) HCASA and (b) SSA

Fig. 11.   The radiation patterns of HCASA (a) E-plane, (b) H-plane, and SSA (c) E-plane, (d) H-plane

respect to the frequency 920MHz. For the same frequency as width, *Ws* is reduced maintaining same h_s value, W_s/h_s is increased. This results in greater surface wave to produce diffraction at the dielectric's edge, contributing to higher cross-polarization levels /16/. It can be realized that the antenna produces almost symmetrical radiation pattern. One of the significant advantages of symmetrical radiation pattern is that the maximum power direction would always be at the boresight direction and would not shift to different

directions at different frequencies. This is why the antenna is greatly suitable for portable omni-directional applications and services.
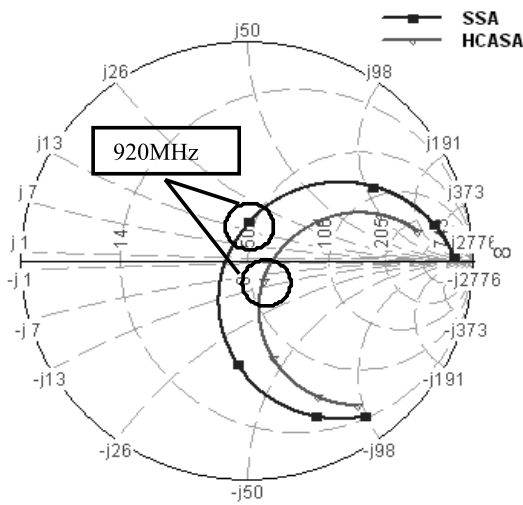

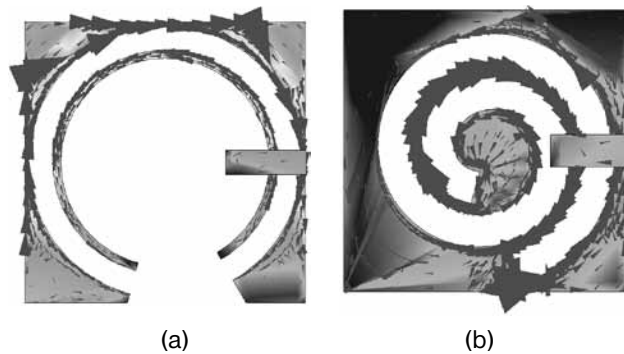Fig. 12. The input impedance of the miniaturized proposed antennas

Fig. 13. The current distribution at 920MHz of proposed (a) HCASA and (b) SSA

The input impedance plots of the microstrip-fed minimized hollow central annular slot antenna (HCASA) and spiral slot antenna (SSA) are depicted in Figure 12. The input

impedance curves change smoothly over the operating frequency. For HCASA, at the resonance the input resistance is about 10Ω more than the SSA. However for SSA the input reactance is mainly inductive. This is for the reason of the spiral slot which acts less capacitive and provides more inductance to the antenna.

The simulated surface current distributions of the compact antennas are illustrated in Figure 13. Arrows show the direction of the current direction. As anticipated from the previous current distributions shown in Figures 3 & 4, critical current flow is observed at the edges of the annular and spiral slots. However it was observed that the current components turn into the reversed direction at the resonant frequencies than lower non-resonating frequencies. The current distributions for the lower non-resonating frequencies are not shown to reduce ingemination and complexity Moreover, at the opposite edges of the slots the currents are in contra-direction to each other.

Finally comparative characteristics of the miniaturized antennas with respect to the conventional reference antenna are provided in Table V. It is obvious from the table that the half circular antennas provide the widest -10dB bandwidths, but the antenna minimization factor is just 53.6%. On the other hand, the reduction factor of finally minimized hollow central annular slot antenna (HCASA) and spiral slot antenna (SSA) are 75 and 86.2%, which makes the antennas extremely compact with respect to the operating frequencies.

7. Conclusion

Increasing demand for smaller size in mobile devices results in a need for effective antenna miniaturization. A technique for miniaturization of slot antennas is presented in this paper. The technique is based on the combination of two different miniaturization techniques: folding of slots and optimizing of the slots keeping the same slot length. Using these techniques, two miniaturized slot antennas, namely hollow central annular slot antenna (HCASA) and spiral slot antenna (SSA) are designed that reduces the volume up to 75 and 86.2% comparing that of an ordinary annular slot

Table 5: Comparison with conventional annular slot antenna and miniaturized antennas

Antenna	Frequency	Return Loss	-10dB return loss bandwidth (MHz)	Dielectric Constant ε_r	Area of the Antenna (mm)	Reduction of antenna area (%)
Conventional Annular Ring Slot Antenna		-10.7	18.2		70×70	Ref. (0%)
Annular Ring Slot Antenna with Side Feeding		-11.5	24.4		70×70	0%
Half Annular Ring Slot Antenna		-18.5	31.7		32.5×70	53.6
Half Double Annular Ring Slot Antenna	920MHz	-20	32.8	4.4	32.5×70	53.6
Half Double Annular Ring Slot Antenna Without Central Disk		-23.5	34.3		32.5×70	53.6
Hollow Central Annular Slot Antenna		-22	20		35×35	75
Spiral Antenna		-19.5	18		26×26	86.2

* Shaded blocks represent measured values

antenna operating at the same frequency. Considering the overall volume of the miniaturized antennas are relatively $0.11\lambda_o \times 0.11\lambda_o \times 0.005\lambda_o$ and $0.08\lambda_o \times 0.08\lambda_o \times 0.005\lambda_o$ where λ_o is the free space operating wavelength. However it is obvious from the analytical parametric study that the antenna can achieve lower frequencies with the same volume which makes the antenna more compact relatively with the resonating wavelength. It was also seen that the compact antennas provides suitable radiation patterns for portable device applications.

References

/1/   Wong, K. L., *Planar antennas for wireless communications*, Hoboken, NJ: J. Wiley and Sons, 2003.

/2/   Karkkakainen, M., and P. Ikonen, "Patch Antenna with Stacked Split-Ring Resonators as an Artificial Magneto-Dielectric Material," *Microwave and Optical Technology Letters*, Vol. 46, 554-556, 2005.

/3/   Wong, K.-L., *Compact and broadband microstrip antennas*, John Wiley & Sons, New York, 2002.

/4/   Bhatti, R.A., Y.-T. Im, and S.-O. Park, "Compact PIFA for Mobile Terminals Supporting Multiple Cellular and Non-Cellular Standards," *IEEE Transactions on Antennas and Propagation,* Vol. 57, No. 9, 2534 - 2540, 2009.

/5/   Wong, K.-L., and C.-H. Huang, "Printed Loop Antenna With a Perpendicular Feed for Penta-Band Mobile Phone Application," *IEEE Transactions on Antennas and Propagation*, Vol. 56, No. 7, 2138 – 2141, 2008.

/6/   Liu, H.-W., and C.-F. Yang, "Miniature PIFA without empty space for 2.4 GHz ISM band applications," *Electronics Letters*, Vol. 46, No. 2, 113 – 115, 2010.

/7/   Wong, K. L., S. W. Su, C. L. Tang, and S. H. Yeh, "Internal shorted patch antenna for a UMTS folder-type mobile phone," IEEE Trans. Antennas Propag., vol. 53, pp. 3391–3394, Oct. 2005.

/8/   Su, S. W. K. L. Wong, C. L. Tang, and S. H. Yeh, "Wideband monopole antenna integrated within the front-end module package," IEEE Trans. Antennas Propag., vol. 54, pp. 1888–1891, Jun. 2006

/9/   James, J.R., and P.S. Hall, *Handbook of microstrip antennas*, London, IEE - Peter Peregrinus, Ltd., 1989.

/10/   Chang, K., and L.-H. Hsieh, *Microwave Ring Circuits and Antennas*, New York: Wiley, 1996.

/11/   Zaker, R., C. Ghobadi, and J. Nourinia, "Bandwidth Enhancement of Novel Compact Single and Dual Band-Notched Printed Monopole Antenna With a Pair of L-Shaped Slots," *IEEE Transactions on Antennas and Propagation*, Vol. 57, No. 12, 3978 – 3983, 2009.

/12/   Behdad, N., and K., Sarabandi, "Slot antenna miniaturization using distributed inductive loading," *IEEE Antennas and Propagation Society International Symposium*, Vol. 1, 308 – 311, 2003.

/13/   Kim, M., H. Choo, and I. Park, "Two-arm microstrip spiral antenna for multi-beam pattern control" *Electronics Letters*, Vol. 41, No. 11, 627 – 629, 2005.

/14/   Mirza, I.O., S. Shi, C. Fazi, J.N. Mait, and D.W. Prather, "A study of loop antenna miniaturization using split ring resonators," *IEEE Antennas and Propagation Society International Symposium*, 1865 – 1868, 2007.

/15/   Delafield, C., and S. Sufyar, "A miniaturization technique of a compact omnidirectional antenna" *3rd European Conference on Antennas and Propagation*, 384 – 388, 2009.

/16/   Chen, I-F., and C.-M. Peng, "A novel reduced size edge-shorted patch antenna for UHF band applications," *IEEE Antennas and Wireless Propagation Letters*, Vol. 8, 475 – 477, 2009.

Ahmed Toaha Mobashsher, Norbahiah Misran

Dept. of Electrical, Electronic and Systems Engineering
Universiti Kebangsaan Malaysia
Bangi, Selangor, Malaysia

Mohammad Tariqul Islam

Institute of Space Science (ANGKASA)
Universiti Kebangsaan Malaysia
Bangi, Selangor, Malaysia